Arab J Geosci (2017) 10: 374
DOI 10.1007/s12517-017-3166-y

ORIGINAL PAPER

Optimization of the Garzan Hydropower System operations

Emrah Yalcin[1] · Sahnaz Tigrek[2]

Received: 1 March 2017 / Accepted: 17 August 2017 / Published online: 25 August 2017

Abstract Through the rapid development of the watersheds in Turkey with projects developed by incorporated companies, a problem has arisen of how to operate a cascade reservoir system composed of state- and private sector-owned reservoirs in terms of the volume and timing of water releases to meet downstream water demands. This study presents a catchment-based optimization model based on inflow forecast with frequent updating for the integrated operation of hydropower plants under various sales methods. The model is formulated in terms of nonlinear programming (NLP) on a monthly basis for a 1-year period to assess the production strategies of the system reservoirs for that year. This model provides the basic constraints on the reservoir volume for daily and hourly optimization procedures. Forecasted flows are generated using seasonal autoregressive integrated moving average (ARIMA) models based on historical flow values. The proposed model is tested on the Garzan Hydropower System using historical, mean, and forecasted flow values. The results show that the integrated operation plan and improvement in the accuracy of inflow forecasts yield economic benefits as a consequence of optimal reservoir operation.

Electronic supplementary material The online version of this article (https://doi.org/10.1007/s12517-017-3166-y) contains supplementary material, which is available to authorized users.

✉ Emrah Yalcin
emrah.yalcin@ahievran.edu.tr

Sahnaz Tigrek
sahnaz.tigrek@batman.edu.tr

[1] Department of Civil Engineering, Ahi Evran University, 40100 Kirsehir, Turkey

[2] Department of Civil Engineering, Batman University, 72100 Batman, Turkey

Keywords Nonlinear programming · Optimization · Reservoir operation · ARIMA · Garzan Basin

Introduction

Growing external energy dependence and rising oil prices are encouraging Turkey to turn to renewable energy, especially hydropower. In this context, the Electricity Market Law No. 4628 and the revised establishment law of the General Directorate of State Hydraulic Works (DSI) No. 6200 gave rise to a new era in the Turkish energy market by transferring the operational rights of existing, under-construction and planned hydropower plants to the private sector and by allocating water rights licenses for the development of new projects for electricity production. Today, through the rapid development of the watersheds with the projects developed by incorporated companies, the problem has arisen of how to operate a cascade reservoir system composed of state- and private sector-owned reservoirs in terms of the volume and timing of water releases to meet downstream water demands.

Power generation companies can sell their electricity through bilateral contracts, the renewable energy sources support mechanism or the day-ahead market operated by the Market Financial Settlement Center (PMUM). Companies have to report their choices of sales method to the Energy Market Regulatory Authority each year. The day-ahead market is the main structure of the energy trade. Producers that prefer to sell electricity on the day-ahead market report their hourly expected production plans to PMUM. Appropriate predictions for the short-term productions of power plants contribute not only to ensuring the system energy balance but also to the profits of companies (Demirdizen 2013).

However, in most of the cascade hydropower systems in the country, a single-reservoir simulation model is employed in the operation of each of the system reservoirs. These model applications are performed with limited knowledge of the short- and long-term operation strategies of the upstream schemes. The administration's influence and control over the basins have loosened as a result of the increasing number of stakeholders involved. The conflicts related to the operation of reservoirs have become increasingly intense with the commissioning of new power plants and irrigation schemes. The situation has resulted in a growing need for an integrated and holistic approach to basin planning and management.

In recent years, basin-wide water resources management tools have been developed for the simulation and optimization of reservoir operations, such as IRAS (Interactive River-Aquifer Simulation), TERRA (Tennessee Valley Authority Environment and River Resource Aid), CTIWM (Cooling Technology Institute Water Management), and RiverWare (Ito et al. 2001). However, these general packages have limited capability in terms of the development of optimal operation policies and water allocation schemes for most site-specific systems (Karamouz et al. 2005). Hence, there is a need to develop site-specific tools to generate decisions in operational management (Rani and Moreira 2010).

Huysentruyt et al. (1996), Karamouz and Zahraie (1996), and Shim et al. (1996) developed decision support systems for power systems in New England, Iran, and South Korea, respectively. Peng (1998) developed a mathematical model for the real-time operation optimization of the West Branch Penobscot River System in the state of Maine of the USA. Barros et al. (2003) formulated a monthly optimization model, called SISOPT, for the management and operation of the Brazilian Hydropower System. Karamouz et al. (2005) presented a system for the monthly operational planning of multipurpose reservoirs in the Dez and Karoon River System in Iran.

This study presents a reservoir system optimization model formulated in terms of nonlinear programming (NLP) for the integrated operation of hydropower plants under various sales methods in the Turkish energy market. The key components of the model are database management, inflow modeling and forecasting, optimization and reservoir operation using inflow forecasts with frequent updating. The assigned system integrates a database with basic hydrological, topographical, and technical information to execute the optimization algorithm. The proposed model is tested on the Garzan Hydropower System using historical, mean, and forecasted flow values for the dry and rainy seasons to analyze its limits and effectiveness in operational management. Moreover, the system reservoirs are operated sequentially using the historical data sets to verify the performance of the integrated operation algorithm against the single-reservoir simulation procedure.

Integrated reservoir system optimization model

Several classical optimization and computational intelligence techniques, such as linear programming, dynamic programming, nonlinear programming, evolutionary computations, fuzzy set theory, and artificial neural networks, have been developed and applied for the management and operations of reservoir systems over the last three decades. Labadie (2004), Rani and Moreira (2010), Wurbs (1993), and Yeh (1985) provided comprehensive literature reviews of the theories and applications of these algorithms in the context of reservoir operation models.

The proposed integrated reservoir system optimization model is formulated in terms of NLP. Although reaching the global optimum is a challenge in NLP, this technique offers the most general formulation of the nonlinear and complex relationships between physical and hydrological variables (Rani and Moreira 2010; Yeh 1985). NLP-based methodologies have additional flexibility with respect to constraint qualifications. This advantage can be put to use in the case of larger, more complex, nonlinear programming problems to obtain well-defined solutions. However, to date, there have been few applications of this technique to hydropower generation because of its extreme computational requirements (Ahmed and Lansey 2001; Kameswaran and Biegler 2008; Rani and Moreira 2010).

The optimization model is established on a monthly basis for a 1-year period to assess the production strategies of the system reservoirs for that year. The suggested system provides the needed 1-year optimal operation policy to make the choice of sales method and the basic constraints on reservoir volume for daily and hourly real-time optimization procedures. The model uses the maximization of income, which is the product of produced energy and energy price, as its objective. Energy production is formulated as a function of net head, power release, and system efficiency, as detailed in Table 1. The constraint set includes flow continuity, turbine capacity, spillway capacity, minimum release, minimum energy production, minimum storage, and reservoir capacity, as listed in Table 2. The distinct feature of the present model that differs from other studies to date is the calculation of the energy production of a cascade hydropower system using inflow forecast with frequent updating. The model uses the advantage of NLP in the formulation of the energy production considering the realistic turbine efficiency and net head values in each time step of the operation period.

Forecasted inflow values are generated using seasonal autoregressive integrated moving average (ARIMA) models based on the historical flow values. ARIMA models have been extensively used for time series forecasting based on only past streamflow values (Maier and Dandy 2000). Fernandez and Vega (2009), Huang et al. (2004), Modarres (2007), Muhamad and Hassan (2005), Wang et al. (2009), and

Table 1 Objective function of the integrated reservoir system optimization model

Objective function	Equation	Symbol	Definition
$\max \sum_t \left[p_t \left(\sum_i E_{i,t} - E^c_t \right) \right]$	(1)	p_t	Estimated energy price for time period t in US dollar cent/kWh
		$E_{i,t}$	Energy production of the ith plant during time period t in kWh
		E^c_t	Contractual energy demand for time period t in kWh
where			
$E_{i,t} = \xi_T \xi_G \varphi_t P_{i,t}$	(2)	ξ_T	Transformer efficiency, 98.5% as default (IFC 2015)
		ξ_G	Generator efficiency, 97.5% as default (IFC 2015)
		φ_t	Conversion factor from time period t to hours
		$P_{i,t}$	Power of the ith plant during time period t in kW
$P_{i,t} = g\, H^n_{i,t} \sum_j \left(\varepsilon_{i,j,t}\, \phi_t\, R^p_{i,j,t} \right)$	(3)	g	Acceleration of gravity, 9.81 m/s^2
		$H^n_{i,t}$	Net head in the ith reservoir during time period t in m
		$\varepsilon_{i,j,t}$	Efficiency of turbine j of the i^{th} reservoir during time period t
		ϕ_t	Conversion factor from m^3 to m^3/s
		$R^p_{i,j,t}$	Power release through the jth turbine of the ith reservoir during time period t in m^3
$\varepsilon_{i,j,t} = f_1\left(\frac{R^p_{i,j,t}}{R^p_{i_{\max}}} \right)$	(4)	$R^p_{i_{\max}}$	Maximum power release through a turbine of the ith reservoir in m^3
		f_1	Fitted curve equation of the relation between the ratio of power release to designed discharge and turbine efficiency
$H^n_{i,t} = \lambda \left(H^a_{i,t} - tw_i \right) - \kappa_i \left(\phi_t \sum_j R^p_{i,j,t} \right)^2$	(5)	λ	Gross head reduction for local losses, 95% as default
		$H^a_{i,t}$	Average water level in the ith reservoir during time period t in m
		tw_i	Tail water level of the ith reservoir
		κ_i	Friction loss constant for the penstocks and/or energy tunnels of the ith reservoir in m/(m^3/s)^2
$H^a_{i,t} = \left(H_{i,t-1} + H_{i,t} \right)/2$	(6)	$H_{i,t-1}$	Water level in the ith reservoir at the beginning of time period t in m
		$H_{i,t}$	Water level in the ith reservoir at the end of time period t in m
$H_{i,t} = f_2(S_{i,t})$	(7)	$S_{i,t}$	Storage in the ith reservoir at the end of time period t in m^3
		f_2	Fitted curve equation of the relation between reservoir storage and water level

Yurekli et al. (2004) provided comprehensive literature reviews of the applications of these models in the context of water resources time series.

Integrated system operation optimizations are performed with these forecasted inflow values for each month of the operation period. The states of the system reservoirs are updated at the beginning of each month based on the observed inflow values of the previous month. If the observed inflow value for a reservoir is lower than its forecasted amount, the spillway release, if any, and then the storage level are decreased at first with the difference of the forecasted and observed flow amounts. In this case, if the changed storage level remains below its minimum value, the optimized power release is decreased until the minimum storage constraint is satisfied. Conversely, if the observed inflow value is higher than its forecasted amount, the storage level is increased by the difference of the observed and forecasted flow amounts. If the increased storage level remains above its maximum value, the optimized power release is increased up to the design discharge, and the remaining storage amount is added to the spillway release. Subsequently, the inflow value of the downstream reservoir is updated based on these adjustments, and the forecasting error modifications are continued for each system reservoir sequentially. The operation optimization for the next month starts with the updated storage levels of the system reservoirs. This procedure is schematically illustrated in Fig. A1 (Online Resource).

The Garzan Hydropower System

The proposed model is applied to the Garzan Hydropower System as a case study. Garzan Creek is a branch of the Tigris River and flows through the south-eastern Anatolia Region of Turkey. The hydropower system consists of the Aysehatun Dam and HEPP Project with the Mutki Derivation, the Kor Dam and HEPP Project, the Garzan Dam and HEPP Project, and the Garzan irrigation scheme, which covers an area of 60,000 ha, as depicted in Fig. 1 (Aksa 2004; DSI 1987; Enersu 2008; Jemas-Su 2001).

The net evaporation rates, monthly mean inflow values, environmental and irrigation water demands, reservoir area

Table 2 Constraint set of the integrated reservoir system optimization model

Constraints	Equation	Symbol	Definition
Flow continuity			
$S_{i,t} = S_{i,t-1} + I_{i,t} + \sum_j R^p_{i-1,j,t} + R^s_{i-1,t} + R^{de}_{i-1,t} + r_{i-1}\, R^{di}_{i-1,t} - e_{i,t}\, A_{i,t-1} - \sum_j R^p_{i,j,t} - R^s_{i,t} - R^{de}_{i,t} - R^{di}_{i,t} - R^{dw}_{i,t}$	(8)	$S_{i,t-1}$	Storage in the *i*th reservoir at the beginning of time period t in m^3
		$I_{i,t}$	Forecasted inflow into the *i*th reservoir during time period t in m^3
		$R^p_{i-1,j,t}$	Power release through the *j*th turbine of the $i-1$th reservoir during time period t in m^3
		$R^s_{i-1,t}$	Non-power release through the spillway from the $i-1$th reservoir during time period t in m^3
		$R^{de}_{i-1,t}$	Non-power release as environmental water from the $i-1$th reservoir during time period t in m^3
		r_{i-1}	Rate of return for the irrigation scheme of the $i-1$th reservoir
		$R^{di}_{i-1,t}$	Irrigation water supplied by the $i-1$th reservoir during time period t in m^3
		$e_{i,t}$	Net evaporation rate per unit area of the *i*th reservoir during time period t in m
		$A_{i,t-1}$	Reservoir area of the *i*th reservoir at the beginning of time period t in m^2
		$R^s_{i,t}$	Non-power release through the spillway from the *i*th reservoir during time period t in m^3
		$R^{de}_{i,t}$	Non-power release as environmental water from the *i*th reservoir during time period t in m^3
		$R^{di}_{i,t}$	Irrigation water supplied by the i^{th} reservoir during time period t in m^3
		$R^{dw}_{i,t}$	Domestic water supplied by the i^{th} reservoir during time period t in m^3
where $A_{i,t-1} = f_3(S_{i,t-1})$	(9)	f_3	Fitted curve equation of the relation between reservoir storage and reservoir area
Turbine capacity			
$R^p_{i,j,t} \le R^p_{i_{\max}}$	(10)		
Spillway capacity			
$R^s_{i,t} \le R^s_{i_{\max}}$	(11)	$R^s_{i_{\max}}$	Spillway capacity of the *i*th reservoir in m^3
Minimum release			
$\sum_j R^p_{i,j,t} + R^s_{i,t} + R^{de}_{i,t} \ge R^d_{i_{\min},t}$	(12)	$R^d_{i_{\min},t}$	Minimum release to supply the water demand from the *i*th reservoir during time period t in m^3
Minimum energy production			
$\sum_i E_{i,t} \ge E^c_t$	(13)		
Minimum and maximum storage values			
$S_{i_{\min}} \le S_{i,t} \le S_{i_{\max}}$	(14)	$S_{i_{\min}}$	Minimum storage in the *i*th reservoir in m^3
		$S_{i_{\max}}$	Maximum storage in the *i*th reservoir in m^3

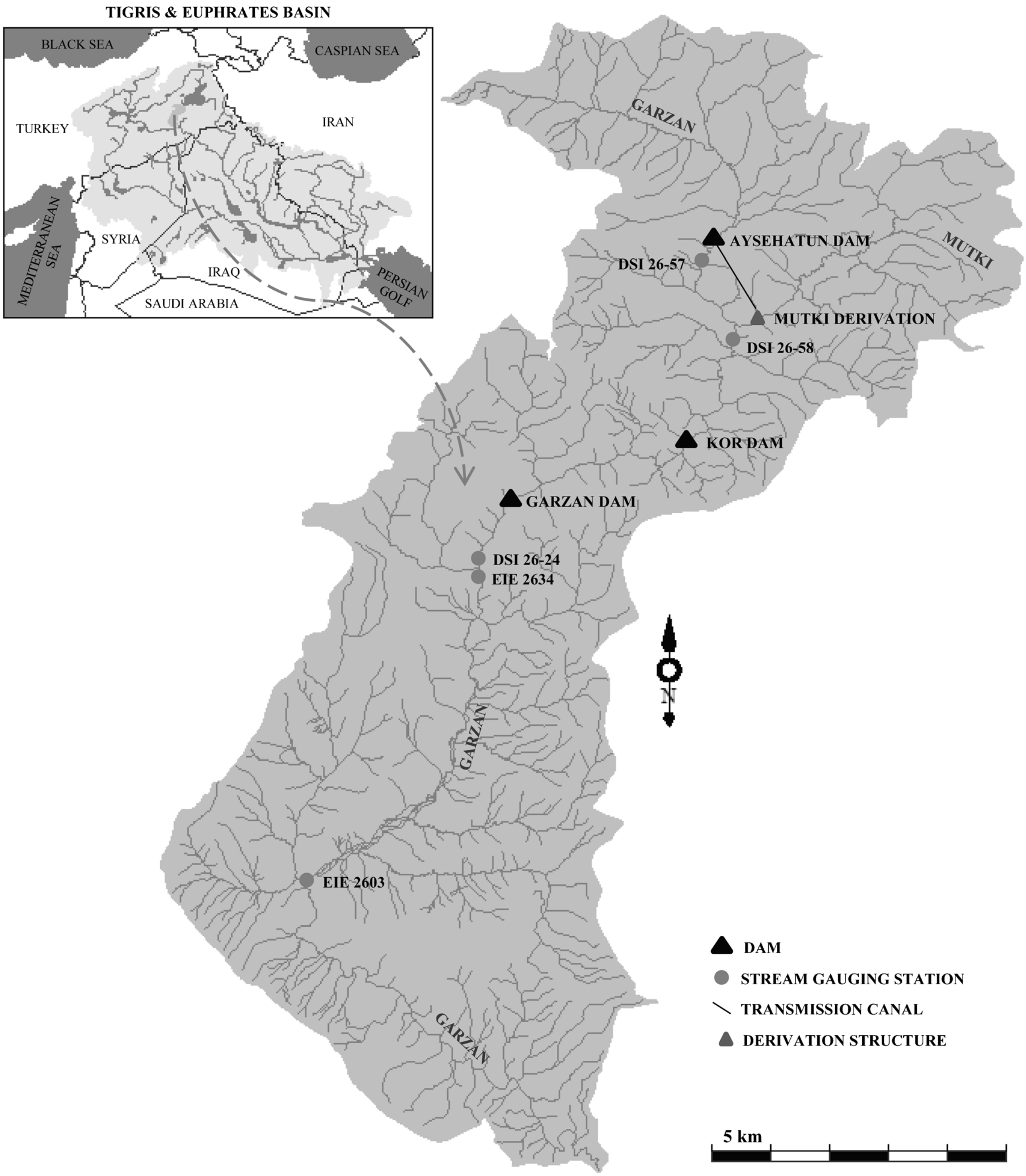

Fig. 1 Location map of the study area

and water level functions expressed as high-order polynomials of the storage, turbine efficiency curves, and energy prices are the inputs to the proposed model, together with the topographical and technical features of the projects, as listed in Table 3 (Yalcin 2015).

The MINOS solver, which employs a projected Lagrangian algorithm on a sequence of linearly constrained sub-problems, is used to solve this optimization problem with nonlinear constraints and the objective function within the General Algebraic Modeling System (GAMS) package (Murtagh et al. 2014). The steps of the procedure followed for this purpose are schematically illustrated in Fig. A2 (Online Resource). Moreover, to verify the efficiency of the integrated operation, the same process is applied to the system reservoirs sequentially.

Evaporation rates

The net evaporation rates of the system reservoirs are based on records from meteorological stations operated by the General Directorate of State Meteorological Works (DMI). For the Aysehatun and Kor projects, the monthly total evaporation

Table 3 Characteristics of the Garzan projects

Characteristics	Unit	Aysehatun	Kor	Garzan
Purpose	–	Energy	Energy	Energy
Drainage area	km^2	405.0	942.2	1266.0
Thalwag elevation	m	1180.0	895.0	675.5
Maximum water level	m	1250.0	956.0	788.3
Minimum water level	m	1230.0	930.0	757.7
Tailwater level	m	950.0	830.0	676.0
Design discharge	m^3/s	13.36	26.54	43.60
Penstock: number/diameter/length	−/m/m	1/2.3/250	1/2.5/210	1/3.2/210
Energy tunnel: number/diameter/length	−/m/m	1/3.5/8410	1/3.3/6370	1/4.0/382
Number of units	–	2	2	2
Gross head/net head	m/m	300.0/282.0	126.0/109.9	112.3/108.6
Turbine type	–	Francis	Francis	Francis

and monthly mean temperature data from the Bitlis meteorological station are used, and for the Garzan Reservoir, the records of the Siirt meteorological station are utilized (DMI 2009). Assuming a 0.5 °C decrease in temperature per 100 m increase in altitude, the temperature data observed at the relevant stations are transformed into the maximum water levels of the reservoirs (Limak 2006). Then, the monthly total evaporation quantities corresponding to these transformed temperatures are determined based on the correlations between the monthly mean temperature and the monthly total evaporation records of these stations. Next, the calculated evaporation values are multiplied by the pan coefficient (0.7) to convert the pan evaporations into the actual evaporation from the lake surface (Usul 2009). Finally, the net evaporation rates per unit area are obtained by subtracting the precipitation records from the appropriate stations from the actual evaporation values. For the Aysehatun and Kor projects, the monthly total precipitation data observed at the Mutki meteorological station are used, and for the Garzan Reservoir, the records from the Kozluk meteorological station are utilized (DMI 2009).

Inflow values

The historical, mean and forecasted flow values for the dry and rainy seasons are provided to the system as input to analyze the limits and effectiveness of the NLP model in operational management. The results of the optimizations based on the historical and mean flow values represent the range of income that can be derived for the period under consideration. In operational studies, the states of the system reservoirs are updated at the beginning of each month due to inflow forecasting errors, and the optimizations are repeated for the remaining portion of the operation period. The increase in the difference between the observed and forecasted flow values requires great modifications in the states of the system reservoirs. These modifications decrease the objective function value that can be achieved at the end of the operation period. The use of the monthly mean flow amounts is the simplest but the least accurate approach in the determination of the forecasted inflow rates. Therefore, whereas the operations based on the historical inflow rates provide an upper bound on the system income, the objective function value based on the monthly mean flow rates can be defined as the lower bound. To investigate how close the results can come to the upper bound, the successively renewed inflow forecasts obtained via seasonal ARIMA models are utilized in the integrated system operation optimizations.

Historical records and averages for months

The monthly mean flow records obtained from the Besiri (EIE 2603), Bogazonu (DSI 26-57), Kozluk (DSI 26-24), Kozluk (EIE 2634), and Meydanonu (DSI 26-58) hydrometric stations operated by DSI and the General Directorate of Electrical Power Resources Survey and Development Administration (EIE) are utilized to investigate the inflow potential at the dam locations (DSI 2007; EIE 2003). These stations are shown in Fig. 1 and are detailed in Table 4.

First, the raw flow data from the Besiri station are corrected for the upstream irrigation abstraction, which covers an area of 3362 ha and has been in operation since 1996, according to the Garzan-Kozluk irrigation module (Enersu 2008). Then, the naturalized flow values and correlations are used to produce representative flow data for the 1971–2000 period. The discontinuities in the records of the Bogazonu and Meydanonu stations are patched based on the correlations with the flow rates of the Besiri gauging station. In the correlation studies, the upstream-downstream relationships along the river branches are evaluated using the quantities for the corresponding months, and inappropriate data sets are not included. In the extension of the flow values measured at the Kozluk (DSI 26-24) station, the correlation equation obtained based on the naturalized flow rates of

Table 4 Characteristics of the stream gauging stations

Station Id	Station name	Opening date	Closing date	Drainage area (km^2)	Elevation (m)	Mean discharge (m^3/s)
DSI 26-57	Keyburan Brook Bogazonu	24.10.1981	–	425.0	1200	8.6
DSI 26-58	Garzan Creek Meydanonu	29.11.1981	08.01.1999	783.2	909	15.8
DSI 26-24	Pisyar Creek Kozluk	01.08.1970	–	1359.3	620	26.0
EIE 2634	Garzan Creek Kozluk	19.10.1999	30.09.2000	1407.7	630	23.0
EIE 2603	Garzan Creek Besiri	01.11.1945	30.09.2000	2450.4	545	49.0

the Besiri gauging station is utilized for the 1985–1999 period. For the year 2000, the quantities are transformed from the observations at the Kozluk (EIE 2634) station based on the catchment area ratio between these stations.

In the estimation of the monthly mean flow rates at the Mutki Weir location, the drainage area ratio among the weir and the intermediate catchment between the Meydanonu and Bogazonu gauging stations is utilized. The amounts diverted from Mutki Creek to Aysehatun Dam are determined from these values according to the transmission canal capacity of 25.74 m^3/s (DSI 1987). The flow rates at the Aysehatun Dam location are converted from the extended data set from the Bogazonu station based on the catchment area ratio between them. The sums of these values with the diverted flows from Mutki Creek are utilized as the observed monthly mean inflow values of the Aysehatun Dam and HEPP Project.

The extended flows of the Meydanonu station are propagated to the Kor Dam site in proportion to the drainage areas. Then, the historical monthly mean inflow values of the Kor Dam and HEPP Project are determined by subtracting the produced runoff values at the Aysehatun Dam and Mutki Weir locations from these values.

The catchment area ratio is used to project the extended runoff rates at the Kozluk (DSI 26-24) gauging station to the Garzan Dam axis. The differences between these values and the flow amounts at the Kor Dam site are treated as the observed monthly mean inflow values of the Garzan Reservoir.

The monthly river flows at the Aysehatun, Kor and Garzan Dam locations for the 30-year period from 1971 to 2000 and their monthly averages are displayed in Fig. A3.a, Fig. A3.b, and Fig. A3.c (Online Resource), respectively. The water years 1988 and 1989 are determined to represent rainy and dry seasons, respectively, according to the statistics of the entire data set and those of the selected test years, as detailed in Table A1 (Online Resource). The averages of the monthly mean flow values for the entire flow record are 35.65, 54.90, and 68.31 hm^3 at the Aysehatun, Kor, and Garzan Dam axes, respectively. These amounts are, in turn, 77.19, 120.87, and 143.70 hm^3 in water year 1988 and 13.37, 20.41, and 24.86 hm^3 in water year 1989. Moreover, the maximum and minimum monthly mean flow amounts are observed in the rainiest and driest water years during the 1971–2000 period, respectively.

Forecasted inflows

ARIMA models, as introduced by Box and Jenkins (1976), are represented by ARIMA $(p, d, q) \times (P, D, Q)_s$. The terms (p, d, q) and $(P, D, Q)_s$ represent the orders of the non-seasonal and seasonal components, respectively, where d is the number of regular differencing; D is the number of seasonal differencing; p is the order of the non-seasonal autoregressive (AR); q is the order of the non-seasonal moving average (MA); P is the order of the seasonal AR; Q is the order of the seasonal MA; and s is the season length, which is 12 for monthly data.

The time series are split into two sets, namely, the training and testing periods. The historical river flow data from 1971 to 1987 and from 1971 to 1988 are used as the training periods for calibrating the forecasting models, and the data from the years 1988 and 1989 are used as the test sets for the verification of the models in the rainy and dry seasons, respectively (Table A1 in Online Resource).

Prior to fitting ARIMA models, the time series are transformed via a logarithmic transformation to eliminate any difficulties arising from non-normality and heteroscedasticity in the estimated residuals (Hipel and McLeod 1994). The autocorrelation functions (ACFs) and partial autocorrelation functions (PACFs) are examined to identify appropriate ARIMA models for the time series of river flows. First, the ACFs are differenced by a lag of 12 because of their seasonality. Then, the presence of non-seasonal and seasonal AR and MA terms in the models is evaluated in accordance with the Akaike information criterion (AIC) and Ljung-Box-Pierce statistics. Finally, the ACFs and PACFs of the residuals are checked to determine whether the residuals lie within confidence limits such that they satisfy the requirements of a white noise process (Shabri and Suhartono 2012).

To determine the forecasted inflow rates for the first month of the operations during the rainy period, the sample ACFs and PACFs of the historical river flow data from 1971 to 1987 are plotted in Fig. A4.a, Fig. A5.a, and Fig. A6.a (Online Resource) for the Aysehatun, Kor, and Garzan Dam locations, respectively. The seasonal spikes do not truncate but rather damp out in the PACFs, and they cut off after a lag of 1 in the ACFs, suggesting that a seasonal MA parameter is needed in the models. Therefore, (P, D, Q) = (0, 1, 1) appears to be appropriate to test as the seasonal component of the models.

However, the non-seasonal patterns in the ACFs and PACFs are not as clear. The patterns could indicate either an MA or an AR parameter. Thus, the non-seasonal component of the models (p, d, q) could be either (1, 0, 0) or (0, 0, 1). Based on the minimum AICs and Ljung-Box-Pierce statistics, the optimal model is the ARIMA (0, 0, 1) $(0, 1, 1)_{12}$ for all dam locations.

The residual plots showing the ACFs and PACFs of the residuals are presented in Fig. A4.b, Fig. A5.b, and Fig. A6.b (Online Resource) for the Aysehatun, Kor, and Garzan Dam locations, respectively. The ACFs and PACFs of the residuals lie within the confidence limits, and the residuals do not exhibit a significant correlation, thereby confirming that the residuals of the selected model are consistent with white noise (Shabri and Suhartono 2012).

The ARIMA models used in each time step of the operations are developed following the same procedure described above using the *IBM SPSS Forecasting* module (IBM Corporation 2012). The selected models are listed in Table A2 (Online Resource).

The observed, mean, and forecasted flow rates at the Aysehatun Dam, Kor Dam, and Garzan Dam locations during the rainy and dry seasons are displayed in Fig. A7 and Fig. A8 (Online Resource), respectively. These graphs show that the ARIMA results are closer to the corresponding observed streamflow values than are the mean inflow rates.

The forecasting performance of the models at the testing stages is evaluated using the mean absolute error (MAE), the root mean square error (RMSE), the mean bias error (MBE), the normalized mean bias error (NMBE), the correlation coefficient (R), and the Nash-Sutcliffe coefficient of efficiency (CE). In addition, the RMSE/^{o} error index, where ^{o} is the mean of the observed flow values, is utilized to compare the results with those of other studies on river flow forecasting (Valipour et al. 2013). Relatively small MAE, RMSE, MBE, and RMSE/^{o} values indicate the accuracy of the forecasting models. The tendency of the models towards over- or under-estimation can be observed from the NMBE values (Ghanbarpour et al. 2009). The R values measure the degree of linear correlation between the predicted and observed flow rates. The CE values provide an indication of the model performance at prediction values far from the mean of the historical time series.

In Table 5, it is shown that for all dam locations and for both seasons, the ARIMA models demonstrate good performance with respect to the monthly averages in the testing phases. Although the mean flow rates are more highly correlated with the observed flows, these increases in the R values have no effect on the magnitudes of the other error measures.

Environmental and irrigation water demands

For the maintenance of natural ecosystems, 10% of the monthly mean inflow values over the last 10 years (1991–2000) is left on the river bed as environmental water due to the energy tunnels of the system projects (DSI 2014). This release is

Table 5 Forecasting performance indices of the mean and ARIMA approaches

Basin	Model	MAE	RMSE	NMBE	RMSE/^{o}	MBE	R	CE
Rainy period								
Aysehatun	Mean	41.541	60.222	− 0.538	0.780	41.541	0.966	0.416
	ARIMA	23.116	39.558	− 0.175	0.512	13.537	0.889	0.748
Kor	Mean	65.973	97.616	− 0.546	0.808	65.973	0.971	0.409
	ARIMA	34.151	57.459	− 0.136	0.475	16.461	0.912	0.795
Garzan	Mean	75.069	104.992	− 0.522	0.731	75.069	0.962	0.446
	ARIMA	49.659	78.018	− 0.049	0.543	7.015	0.876	0.694
Dry period								
Aysehatun	Mean	22.369	38.555	1.666	2.884	− 22.277	0.630	− 9.608
	ARIMA	13.230	19.670	0.586	1.471	− 7.838	0.468	− 1.761
Kor	Mean	34.645	59.526	1.690	2.917	− 34.494	0.632	− 9.337
	ARIMA	28.643	47.341	0.811	2.320	− 16.554	0.382	− 5.538
Garzan	Mean	44.069	74.337	1.761	2.991	− 43.774	0.646	− 7.742
	ARIMA	35.134	52.321	0.787	2.105	− 19.566	0.355	− 3.331

formulated in the model through the inclusion of the term R^{de} in the flow continuity equation defined in Table 2.

The Garzan irrigation scheme is largely sourced from the outflows of the Garzan Reservoir. Hence, operations must be conducted such that the outflow rates are equal to or greater than the irrigation water demands of the corresponding months, which are determined in accordance with the Garzan irrigation module (FPGA 1968). In the model, the minimum release constraint defined in Table 2 guarantees that the irrigation demand will be met through the outflows of the Garzan Reservoir.

Turbine efficiency

Turbine efficiency depends on the type of turbine and the ratio of power release to capacity. The efficiency curves for Francis-type turbines, which are the type utilized in the system power plants, are defined in the model as high-order polynomials of the ratio of the power release to the designed discharge (Pro-sem 2008; Yalcin 2015).

Energy prices

There are two types of prices on the day-ahead market, namely, the market-clearing price (MCP) and the system marginal price (SMP). If a producer supplies its expected amount of produced energy on time, as previously reported to PMUM, it receives payment at the MCP. If the produced energy is more or less than the reported amount, it leads to a system imbalance, and the SMP enters the calculation (Demirdizen 2013). The MCP and SMP averages and the averages for months are presented in Fig. A9 and Fig. A10 (Online Resource), respectively.

The day-ahead market has been in operation since December 2009 (PMUM 2014). There are not sufficient data available to apply a monthly forecasting procedure. Hence, the monthly SMP averages are utilized as inputs to the NLP model.

Operational studies

Optimization studies are performed for the rainy and dry seasons using three different inflow sets. The initial and ending storage values of the system reservoirs are constrained to be equal to the dead volumes. In addition, the contractual energy demand is not considered, and the operations are optimized using a model that assumes that all produced energy will be sold on the day-ahead market (Yalcin 2015).

The operations based on the historical inflow rates provide an upper bound on the income that can be obtained for the period under consideration. Moreover, the system reservoirs are operated sequentially using the historical data sets to evaluate the efficiency of the integrated operation plan. In these consecutive operations, the inflow values are obtained by adding the optimized outflows of the upstream projects to the intermediate basin flows.

Then, the monthly means of the extended data sets from 1971 to 2000 are utilized as input during the 12-month operation period for each fall season. These objective function values can be defined as the lower bounds on the combined system incomes. The optimizations are repeated 12 times at the beginning of each month based on the real states of the system reservoirs.

To provide an estimate of income that can be achieved in practice, the same procedure is performed using the successively renewed inflow forecasts obtained via the selected ARIMA models. The states of the system reservoirs are updated at the beginning of each month based on the observed inflow values from the previous month.

Rainy season operations

The objective function values for the combined and separate system operations based on the historical time series are presented in Fig. A11 (Online Resource). The total income for the integrated system operation is 55.57 million US dollars/year. According to the results of the sequential optimization studies of the system reservoirs, the income during the period under consideration is 52.14 million US dollars/year. Therefore, for the same period of operation with the same initial and ending storage values, the integrated optimization model yields 6.59% more revenue than the separate reservoir optimization approach (Table 6).

Figure A12 (Online Resource) presents a comparison of the monthly storage variations of the system reservoirs, and Fig. A13 (Online Resource) shows a comparison of the income values obtained from three different inflow series. The NLP model based on the historical inflow rates yields 5.34% more income than the model based on the mean inflow values and 3.66% more income than the model based on the forecasting results (Table 6). The reason for this difference is based on the amounts of spilled water for the Garzan Reservoir, as presented in Fig. A14 (Online Resource).

Table 6 Results of the operations for the Garzan Hydropower System

Income (million US dollar)		Aysehatun	Kor	Garzan	Total
Rainy period					
Combined system run	Historical	20.05	13.74	21.78	55.57
	Mean	19.47	13.55	19.74	52.76
	Forecasted	19.69	13.71	20.21	53.61
Separate system runs	Historical	20.22	13.11	18.81	52.14
Dry period					
Combined system run	Historical	6.40	3.34	5.50	15.24
	Mean	Infeasible			
	Forecasted	Infeasible			
Separate system runs	Historical	6.67	3.49	5.00	15.16

Dry season operations

In water year 1989, the critical factor is the irrigation water needs of the Garzan irrigation scheme. In this year, 215.14 hm^3 of water must be supplied from the outflows of the Garzan Reservoir, but the total flow volume of the intermediate basin between the Kor and Garzan reservoirs is only 59.21 hm^3. Therefore, the outflow of the Kor HEPP is critical for satisfying the irrigation water demand.

The income value of the combined system for water year 1989 is 15.24 million US dollars/year. However, in the sequential optimization studies of the system reservoirs, the Garzan Reservoir operation optimization does not converge because of the minimum release constraint defined in Table 2. This outcome is likely to occur in real-life applications during such a dry season when all reservoirs and the irrigation scheme are in operation. By decreasing the demand amounts until convergence is reached, the optimization becomes feasible at 83% of the initial demand, and the total income of the reservoir system is 15.16 million US dollars/year (Fig. A15 in Online Resource). Comparisons of the income values obtained from the combined and separate system operations and the monthly storage variations of the system reservoirs are presented in Fig. A16 and Fig. A17 (Online Resource), respectively.

The same situation is also observed in the operation optimizations when the monthly mean and forecasted flow values are taken as inputs to the model. The NLP model, considering the system as a whole, begins to fail to converge after several steps. The optimization does not converge in run-8 (May to September) using the mean flow values or in run-5 (February to September) using the updated ARIMA forecasts. The reason for these non-convergences is that insufficient storage is allocated for the irrigation needs because of the inadequate inflow values.

Discussions

The proposed site-specific optimization model is utilized to verify the performance of the catchment-based operation algorithm against the sequential optimization of the system reservoirs. This model gives the opportunity to conduct a realistic comparison in terms of system income by means of the advantage of NLP in the formulation of energy production. The integrated and sequential optimization studies are conducted with the historical inflow data sets of the rainiest and driest water years during the 1971–2000 period. For both fall seasons, the integrated system operation plans yield more income than do the sequential optimization studies of the system reservoirs (Table 6). Moreover, in the dry season, the sequential system operation plans generate insufficient outflow rates that satisfy only 83% of the downstream irrigation demand.

The optimization results based on the historical inflow values are the upper bounds of the system income. These results cannot be reached in real-life management practices due to unknown inflow conditions. To investigate how close the results can come to this theoretical upper bound, the integrated system operations are performed for each fall season with the successively renewed inflow forecasts and the monthly means of the historical inflow data sets. In the rainy season, the operations based on the ARIMA forecasts and the mean inflow values supply 96.34 and 94.66% of the revenue optimized using the integrated algorithm with the historical inflow rates, respectively. However, in the dry season, the operation optimizations begin to fail to converge after several steps when the monthly mean and forecasted flow values are taken as inputs to the model. These findings illustrate the importance of forecasts to real-life operational management practices. The CE and R values of the ARIMA forecasts and the mean flow rates are indicators of this result. The negative CE values indicate that the observed mean is a better predictor than the forecasting model results (Table 5).

Although there are 30-year historical inflow data, the model is tested only for the rainiest and driest water years to evaluate the forecasting performance of the ARIMA models and its effectiveness in operational management. The results show that the ARIMA models fail in forecasting the inflow rates in the driest water year coming just after the rainiest water year of the observation period. To enhance the forecasting performance of the ARIMA models, other hydroclimatic data, including precipitation, temperature, and evaporation, can be integrated as independent variables. Moreover, other techniques for streamflow forecasting, such as least-squares support vector machine (LSSVM), artificial neural network (ANN), and support vector machine (SVM) models, can be integrated into the optimization system to achieve more accurate estimates (Shabri and Suhartono 2012).

This monthly operation algorithm must be adapted to daily and hourly real-time optimizations based on the floating energy prices on the day-ahead market (PMUM 2014). After the determination of a 1-year monthly optimal operation policy in terms of the volume and timing of water releases to meet the downstream water demands, the integrated daily and hourly real-time operation optimization studies must be conducted according to the basic constraints on reservoir volume obtained by means of the monthly operation optimization of reservoir systems. This process is indispensable to prevent energy imbalances and enormous price differences on the day-ahead market and to increase the economic benefits of stakeholders.

Furthermore, the concept of firm energy can be used to maximize the reliable energy production capacity obtainable on a long-term basis, even during the most adverse hydrological seasons (Ouarda et al. 1997). In this context, the objective function of the proposed model can be modified to maximize the total energy production. In addition, the power-release terms in the constraints are expressed in terms of the sum of the firm and secondary power releases. The results of such an examination can be utilized to establish energy contracts, and significantly higher revenues can be obtained than with the day-ahead market. Moreover, basin projects can be analyzed under various hydrological scenarios to assess the results of delaying or advancing the schedule of a power plant, expanding the capacity of existing plants or adjusting the normal and minimum operating levels of system reservoirs.

Conclusions

Integrated reservoir operation is important for hydropower system reservoirs from which water is subtracted for agriculture activities, human settlements, and industrial needs. Particularly, in a cascade system composed of state- and private sector-owned reservoirs, the manner in which reservoirs are operated in terms of the volume and timing of water releases to meet downstream water supply demands is a problem of some concern.

In this context, it is demonstrated in this study that an integrated operation plan and adequate flow forecasts make a beneficial contribution to the effective management of the incoming water and, thus, the energy production. When the performance of the integrated algorithm is verified against the sequential optimization of the system reservoirs, the catchment-based optimization model produces more energy by maximizing head and minimizing spill and supplies the irrigational water demand even under the most adverse climatic conditions. Moreover, it is revealed that improvement in the accuracy of the forecasts used in real-life management practices yields economic benefits as a consequence of optimal reservoir operation. Even a small percentage increase in energy production is substantial.

Consequently, cascade hydropower systems, for which single-reservoir simulation models are employed in the operation of each of the system reservoirs, as in the case of Turkey, must be planned and operated through an integrated management process to use hydropower potential more efficiently. The application of such a process reduces conflicts and increases benefits because “the whole is greater than the sum of its parts” (Barrow 2001).

References

Ahmed I, Lansey KE (2001) Optimal operation of multi-reservoir systems under uncertainty. In: Phelps D, Shelke G (eds) Proceedings of world water and environmental resources congress: bridging the gap, meeting the world’s water and environmental resources challenges. ASCE, Orlando, pp 1–9

Aksa (Aksa Energy Generation Incorporated Company) (2004) Kor Barajı ve HES fizibilite raporu. Aksa

Barros MTL, Tsai FT, Yang S, Lopez JEG, Yeh WW (2003) Optimization of large-scale hydropower system operations. J Water Res Pl-ASCE 129(3):178–188. https://doi.org/10.1061/(ASCE)0733-9496(2003)129:3(178)

Barrow CJ (2001) A review of the global experience of integrated river basin development planning and management. In: Biswas AK, Tortajada C (eds) Integrated river basin management: the Latin American experience. Oxford University Press, New Delhi, pp 1–30

Box GEP, Jenkins GM (1976) Time series analysis: forecasting and control. Holden-Day, San Francisco

Demirdizen HG (2013) Market development of renewable energy in Turkey (Master’s thesis). Middle East Technical University, Ankara

DMI (General Directorate of State Meteorological Works) (2009) Monthly total precipitation, monthly mean temperature and monthly total evaporation records. DMI, Ankara

DSI (General Directorate of State Hydraulic Works) (2007) Akım gözlem istasyonları: Aylık toplam akımlar (1954–2000). DSI, Ankara

DSI (General Directorate of State Hydraulic Works) (2014) http://www.dsi.gov.tr/. Accessed 25 May 2014

DSI (XVII th Regional Directorate of State Hydraulic Works) (1987) Bitlis-Garzan Projesi: Ayşehatun Barajı ve HES planlama raporu. DSI, Van

EIE (General Directorate of Electrical Power Resources Survey and Development Administration) (2003) Aylık ortalama akımlar (1935–2000). EIE, Ankara

Enersu (Enersu Engineering Consultancy Construction Industry and Trade Limited Company) (2008) Garzan Barajı ve HES revize fizibilite raporu. Enersu, Ankara

Fernandez C, Vega JA (2009) Streamflow drought time series forecasting: a case study in a small watershed in North West Spain. Stoch Env Res Risk A 23(8):1063–1070. https://doi.org/10.1007/s00477-008-0277-8

FPGA (Euphrates Planning Group Authority) (1968) Dicle Havzası istikşaf raporu. FPGA, Diyarbakir

Ghanbarpour MR, Abbaspour KC, Hipel KW (2009) A comparative study in long-term river flow forecasting models. Intl J River Basin Management 7(4):403–413. https://doi.org/10.1080/15715124.2009. 9635398

Hipel KW, McLeod AI (1994) Time series modelling of water resources and environmental systems. Elsevier, Amsterdam

Huang W, Xu B, Chan-Hilton A (2004) Forecasting flow in Apalachicola River using neural networks. Hydrol Process 18(13):2545–2564. https://doi.org/10.1002/hyp.1492

Huysentruyt J, Olason T, Bridgeman S, Allen R (1996) Hydroelectric generation scheduling for the Connecticut and Deerfield river systems. Proceedings of 5th Water Resources Operation Management Workshop. ASCE, New York, pp 209-216

IBM Corporation (2012) IBM SPSS forecasting. http://public.dhe.ibm.com/common/ssi/ecm/yt/en/ytd03018usen/YTD03018USEN.PDF. Accessed 10 January 2015

IFC (International Finance Corporation) (2015) Hydroelectric power: a guide for developers and investors. http://www.ifc.org/wps/wcm/connect/topics_ext_content/ifc_external_corporate_site/ifc+sustainability/learning+and+adapting/knowledge+products/publications/hydroelectric_power_a_guide_for_developers_and_investors. Accessed 10 March 2015

Ito K, Xu ZX, Jinno K, Kojiri T, Kawamura A (2001) Decision support system for surface water planning in river basins. J Water Res Pl-ASCE 127(4):272–276. https://doi.org/10.1061/(ASCE)0733-9496(2001)127:4(272)

Jemas-Su (Jemas-Su Groundwater Survey and Engineering Limited Company) (2001) Bitlis-Garzan Projesi: 1987 yılında hazırlanan Ayşehatun Barajı ve HES planlama raporunun revize bölümleri. Jemas-Su, Ankara

Kameswaran S, Biegler LT (2008) Advantages of nonlinear-programming-based methodologies for inequality path-constrained optimal control problems: a numerical study. SIAM J Sci Comput 30(2):957–981. https://doi.org/10.1137/050644938

Karamouz M, Zahraie B (1996) Water resources management of Tehran metropolitan area: a decision support system (DSS). Proceedings of 5th Water Resources Operation Management Workshop. ASCE, New York, pp 348-360

Karamouz M, Zahraie B, Araghinejad S (2005) Decision support system for monthly operation of hydropower reservoirs: a case study. J Comput Civ Eng 19(2):194–207. https://doi.org/10.1061/(ASCE)0887-3801(2005)19:2(194)

Labadie JW (2004) Optimal operation of multireservoir systems: state-of-the-art review. J Water Res Pl-ASCE 130(2):93–111. https://doi.org/10.1061/(ASCE)0733-9496(2004)130:2(93)

Limak (Limak Hydropower Plant Investments Incorporated Company) (2006) Alkumru Barajı ve HES Projesi fizibilite raporu. Limak, Ankara

Maier HR, Dandy GC (2000) Neural networks for the production and forecasting of water resource variables: a review and modelling issues and application. Environ Model Softw 15(1):101–124. https://doi.org/10.1016/S1364-8152(99)00007-9

Modarres R (2007) Streamflow drought time series forecasting. Stoch Env Res Risk A 21(3):223–233. https://doi.org/10.1007/s00477-006-0058-1

Muhamad JR, Hassan JN (2005) Khabur River flow using artificial neural networks. Al-Rafidain Eng 13(2):33–42

Murtagh BA, Saunders MA, Murray W, Gill WE (2014) MINOS solver manual http://www.gams.com/dd/docs/solvers/minos.pdf. Accessed 12 October 2014

Ouarda TBMJ, Labadie JW, Fontane DG (1997) Indexed sequential hydrologic modeling for hydropower capacity estimation. J Am Water Res Assoc 33:1337–1349. https://doi.org/10.1111/ j.1752-1688.1997.tb03557.x

Peng C (1998) Dynamic operation of a reservoir system with discontinuous and short-term data (Doctoral thesis). University of Arizona, Arizona

PMUM (Market Financial Settlement Centre)(2014) Market clearing price (MCP) and system marginal price (SMP) averages. https://rapor.pmum.gov.tr/rapor/xhtml/ptfSmfDonemlik.xhtml. Accessed 14 November 2014

Pro-sem (Pro-sem Engineering Architecture Consultancy Limited Company) (2008) Pülümür Barajı ve HES fizibilite raporu. Pro-sem, Ankara

Rani D, Moreira MM (2010) Simulation-optimization modelling: a survey and potential application in reservoir systems operation. Water Resour Manag 24:1107–1138. https://doi.org/10.1007/s11269-009-9488-0

Shabri A, Suhartono (2012) Streamflow forecasting using least-squares support vector machines. Hydrolog Sci J 57(7):1275–1293. https://doi.org/10.1080/02626667.2012.714468

Shim SB, Fontane D, Lee HS, Koh DK (1996) Decision support systems in Han River Basin, South Korea. Proceedings of 5th Water Resources Operation Management Workshop. ASCE, New York, pp 67-84

Usul N (2009) Engineering hydrology. METU Press, Ankara

Valipour M, Banihabib ME, Behbahani SME (2013) Comparison of the ARMA, ARIMA, and the autoregressive artificial neural network models in forecasting the monthly inflow of Dez Dam Reservoir. J Hydrol 476:433–441. https://doi.org/10.1016/j.jhydrol.2012.11.017

Wang WC, Chau KW, Cheng CT, Qiu L (2009) A comparison of performance of several artificial intelligence methods for forecasting monthly discharge time series. J Hydrol 374(3–4):294–306. https://doi.org/10.1016/j.jhydrol.2009.06.019

Wurbs RA (1993) Reservoir-system simulation and optimization models. J Water Res Pl-ASCE 119(4):455–472. https://doi.org/10.1061/(ASCE)0733-9496(1993)119:4(455)

Yalcin E (2015) Optimisation of the Tigris River Hydropower System operations (Doctoral thesis). Middle East Technical University, Ankara

Yeh WW-G (1985) Reservoir management and operations models: a state-of-the-art review. Water Resour Res 21(12):1797–1818

Yurekli K, Kurunc A, Simsek H (2004) Prediction of daily streamflow based on stochastic approaches. J Spat Hydrol 4(2):1–12